



*J. Serb. Chem. Soc.* 75 (4) 459–473 (2010)  
JSCS-3979

# Journal of the Serbian Chemical Society

JSCS@tmf.bg.ac.rs • www.shd.org.rs/JSCS

UDC 546.11+547.581.2:541.49:548.7

Original scientific paper

## Crystal engineered acid–base complexes with 2D and 3D hydrogen bonding systems using *p*-hydroxybenzoic acid as the building block

PU SU ZHAO\*, XIAN WANG, FANG FANG JIAN, JUN LI ZHANG and HAI LIAN XIAO

New Materials and Function Coordination Chemistry Laboratory, Qingdao University of Science and Technology, Qingdao Shandong 266042, P. R. China

(Received 16 April, revised 21 September 2009)

**Abstract:** *p*-Hydroxybenzoic acid (*p*-HOBA) was selected as the building block for self-assembly with five bases, *i.e.*, diethylamine, *tert*-butylamine, cyclohexylamine, imidazole and piperazine, and generation of the corresponding acid–base complexes **1–5**. Crystal structure analyses suggest that proton-transfer from the carboxyl hydrogen to the nitrogen atom of the bases can be observed in **1–4**, while only in **5** does a solvent water molecule co-exist with *p*-HOBA and piperazine. With the presence of O–H···O hydrogen bonds in **1–4**, the deprotonated *p*-hydroxybenzoate anions (*p*-HOBAA<sup>−</sup>) are simply connected each other in a head-to-tail motif to form one-dimensional (1D) arrays, which are further extended to distinct two-dimensional (2D) (for **1** and **4**) and three-dimensional (3D) (for **2** and **3**) networks via N–H···O interactions. While in **5**, neutral acid and base are combined pair-wise by O–H···N and N–H···O bonds to form a 1D tape and then the 1D tapes are sequentially combined by water molecules to create a 3D network. Some interlayer or intralayer C–H···O, C–H···π and π···π interactions help to stabilize the supramolecular buildings. Melting point determination analyses indicate that the five acid–base complexes are not the ordinary superposition of the reactants and they are more stable than the original reactants.

**Keywords:** hydrogen bonding; crystal structure; supramolecular; *p*-hydroxybenzoic acid.

### INTRODUCTION

Organic crystals built from acid–base complexes have received considerable attention in the predictable assembly of supramolecular architectures.<sup>1–7</sup> One of the important ways is the use of self-organization of small molecules with N–H···O, O–H···O and other weak intermolecular interactions to create one-, two-, and three-dimensional (1D, 2D, and 3D) networks in crystalline solids.<sup>8,9</sup> Recent

\*Corresponding author. E-mail: zhaopusu@163.com  
doi: 10.2998/JSC090416011Z

studies were focused on the host networks with space to create materials for molecular storage and catalysis.<sup>10–12</sup> In the context of designing specific arrays, aromatic acid molecules attract great interest because of their importance in crystal engineering, due to their ability to form strong and directional hydrogen bond,<sup>12</sup> whereby the number of carboxylic groups and the different placement of the carboxylic group on the aromatic ring may lead to variable hydrogen-bonding fashions and architectures. For example, 3,5-dinitrobenzoic acid, terephthalic acid, trimelic acid and benzene-1,2,4,5-tetracarboxylic acid were successfully employed as building blocks to construct various hydrogen-bond supramolecules.<sup>1,13–15</sup> Among numerous aromatic acids, *p*-hydroxybenzoic acid (*p*-HOBA) is a typical monocarboxylic acid. Although a dimer can be formed by *p*-HOBA itself,<sup>16</sup> using this synthon with organic bases, such as pyridine,<sup>17</sup> pyrrolidine,<sup>18</sup> benzylamine,<sup>19</sup> *N,N*-dimethylbenzylamine,<sup>19</sup> *N*-methylbenzylamine,<sup>19</sup> and (*S*)-1-ethylphenylamine,<sup>20</sup> more organic crystals were reported. In early reports,<sup>18,19</sup> *p*-hydroxybenzoic acid (*p*-HOBA) was always deprotonated as the *p*-hydroxybenzoate anion (*p*-HOBA<sup>–</sup>) and the corresponding organic bases were always protonated, which means an increase of the hydrogen bond acceptor sites in *p*-HOBA and the increase of the hydrogen bond donor sites in the organic bases. Thus, the numbers and varieties of the hydrogen bond between *p*-HOBA and the organic bases will increase, which will finally form rich hydrogen bonding systems and help in the building of multiple hydrogen-bond networks. With this in mind, *p*-hydroxybenzoic acid (*p*-HOBA) was chosen as a building block to construct organic crystals with various organic bases. It is imaginable that combinations of the *p*-HOBA molecule with different organic bases will exhibit variable hydrogen bonding modes and interesting networks. Herein, the synthesis and the molecular structures, as well as the supramolecular structures of complexes formed by *p*-HOBA with the organic bases of diethylamine, *tert*-butylamine, cyclohexylamine, imidazole and piperazine are described.

## EXPERIMENTAL

### Materials and methods

All employed chemicals were of analytical reagent grade purchased from Sinopharm Chemical Reagent Co. Ltd., P. R. China, and used directly without further purification. Elemental analyses for carbon, hydrogen and nitrogen were performed using a Perkin–Elmer 240C elemental instrument. The melting points were determined on a Yanaco MP-500 melting point apparatus. The IR spectra were recorded in the wavenumber range 4000–400 cm<sup>–1</sup> using KBr pellets on a Nicolet 170SX spectrophotometer.

### Synthesis of the compounds

[*p*-HOBA<sup>–</sup>]<{protonated diethylamine} (**1**). *p*-HOBA (276 mg, 2.00 mmol) was dissolved in a mixture of water (10.0 mL) and ethanol (10.0 mL) with stirring and then transferred into a straight glass tube. Diethylamine (0.20 mL, 2.0 mmol) was carefully layered onto it. Colorless block crystals were observed on the tube wall after 2 days.

[p-HOBA<sup>-</sup>]-[protonated tert-butylamine] (**2**). p-HOBA (276 mg, 2.00 mmol) was dissolved in a mixture of water (10.0 mL) and ethanol (10.0 mL) with stirring and then transferred into a straight glass tube. *tert*-Butylamine (0.21 mL, 2.0 mmol) was carefully layered onto it. Colorless block crystals were observed on the tube wall after 3 days.

[p-HOBA<sup>-</sup>]-[protonated cyclohexylamine] (**3**). The same procedure as for **1** was applied except cyclohexylamine (0.23 mL, 2.0 mmol) was used instead of diethylamine and colorless block crystals were obtained after 2 days.

[p-HOBA<sup>-</sup>]-[protonated imidazole] (**4**). p-HOBA (276 mg, 2.00 mmol) and imidazole (136 mg, 2.00 mmol) were dissolved in a mixture of water (10.0 mL) and ethanol (10.0 mL) under stirring. Upon slow evaporation of the solvents at room temperature, colorless block single crystals suitable for X-ray analysis were obtained after 4 days.

[p-HOBA]-[piperazine]-H<sub>2</sub>O (**5**). p-HOBA (276 mg, 2.00 mmol) and piperazine (172 mg, 2.00 mmol) were dissolved in a mixture of water (10.0 mL) and ethanol (10.0 mL) under stirring. Upon slow evaporation of the solvents at room temperature, colorless block single crystals suitable for X-ray analysis were obtained after 4 days.

#### *Single-crystal X-ray diffraction studies*

The diffraction data for **1–5** were collected on an Enraf-Nomius CAD-4 diffractometer with graphite-monochromated MoK $\alpha$  radiation ( $\lambda = 0.71073 \text{ \AA}$ ,  $T = 293 \text{ K}$ ) in the  $\omega$ -scan mode. The structures were solved by direct methods and refined by least squares on  $F^2$  using the SHELXTL<sup>21</sup> software package. All non-hydrogen atoms were anisotropically refined. The positions of the hydrogen atom were fixed geometrically at calculated distances and allowed to ride on the parent carbon atoms. The molecular graphics were plotted using SHELXTL. Atomic scattering factors and anomalous dispersion corrections were taken from the International Tables for X-ray Crystallography.<sup>22</sup> Further detailed information of the crystallographic data and structural analysis for **1–5** are listed in Table I.

TABLE I. Crystal data and structure refinement summary for compounds **1–5**

Property	<b>1</b>	<b>2</b>	<b>3</b>	<b>4</b>	<b>5</b>
Empirical formula	C <sub>11</sub> H <sub>17</sub> NO <sub>3</sub>	C <sub>11</sub> H <sub>17</sub> NO <sub>3</sub>	C <sub>13</sub> H <sub>19</sub> NO <sub>3</sub>	C <sub>10</sub> H <sub>10</sub> N <sub>2</sub> O <sub>3</sub>	C <sub>9</sub> H <sub>13</sub> NO <sub>4</sub>
$M_r$	211.26	211.26	237.29	206.20	199.20
Crystal size, mm	0.24×0.20×0.16	0.24×0.22×0.18	0.22×0.20×0.18	0.26×0.18×0.14	0.22×0.20×0.16
Crystal system	Orthorhombic	Monoclinic	Monoclinic	Monoclinic	Monoclinic
Space group	<i>Pbca</i>	<i>P2<sub>1</sub>/c</i>	<i>P2<sub>1</sub>/c</i>	<i>P2<sub>1</sub>/c</i>	<i>P2<sub>1</sub>/c</i>
<i>a</i> / Å	12.176(2)	6.8300(14)	6.1820(12)	9.6160(19)	6.6120(13)
<i>b</i> / Å	10.728(2)	9.2790(19)	14.184(3)	10.587(2)	11.898(2)
<i>c</i> / Å	17.666(4)	19.831(4)	15.038(3)	11.075(5)	12.442(3)
$\alpha$ / °	90	90	90	90	90
$\beta$ / °	90	99.58(3)	99.74(3)	118.93(2)	92.48(3)
$\gamma$ / °	90	90	90	90	90
<i>V</i> / Å <sup>3</sup>	2307.6(8)	1239.3(4)	1299.6(5)	986.8(5)	977.9(3)
<i>Z</i>	8	4	4	4	4
$\rho_{\text{calcd}}$ / g cm <sup>-3</sup>	1.216	1.132	1.213	1.388	1.353
<i>F</i> (000)	912	456	512	432	424
$\mu$ / mm <sup>-1</sup>	0.088	0.082	0.086	0.105	0.107



TABLE I. Continued

Property	<b>1</b>	<b>2</b>	<b>3</b>	<b>4</b>	<b>5</b>
$\theta$ Range, °	2.31–26.95	2.08–26.96	1.99–27.01	2.42–26.96	2.37–26.97
Completeness to $\theta$ , %	98.2	99.3	97.5	97.9	97.1
Range of $h, k, l$	-14/14, -12/0, -21/0	0/8, 0/11, -23/23	0/7, -16/16, -17/17	0/11, -12/0, -14/12	0/7, 0/14, -14/14
Reflections collected/unique	4815/2468	2899/2677	5895/2766	2232/2109	2245/2071
$R_{\text{int}}$	0.0789	0.0391	0.0735	0.0268	0.0215
Data/restraints/parameters	2468/0/205	2677/0/149	2766/0/167	2109/0/137	2071/1/140
GOF on $F^2$	0.946	1.046	0.997	1.063	1.073
Final $R$ indices ( $I > 2\sigma(I)$ )	$R_1 = 0.0432$ , $wR_2 = 0.0847$	$R_1 = 0.0567$ , $wR_2 = 0.1456$	$R_1 = 0.0527$ , $wR_2 = 0.1273$	$R_1 = 0.0388$ , $wR_2 = 0.1039$	$R_1 = 0.0551$ , $wR_2 = 0.1662$
$R$ indices (all data)	$R_1 = 0.1610$ , $wR_2 = 0.1100$	$R_1 = 0.0883$ , $wR_2 = 0.1700$	$R_1 = 0.1307$ , $wR_2 = 0.1604$	$R_1 = 0.0641$ , $wR_2 = 0.1150$	$R_1 = 0.0672$ , $wR_2 = 0.1766$
Extinction coefficient	0.0112(12)	0.59(3)	0.018(3)	0.022(3)	0.074(11)
Peak, hole $\text{e}\text{\AA}^{-3}$	0.124, -0.114	0.217, -0.294	0.227, -0.261	0.219, -0.185	0.615, -0.662

## RESULTS AND DISCUSSION

*Preparation of compounds 1–5*

Since *p*-HOBA is only slightly soluble in water but well soluble in ethanol, and the organic bases used in this work easily dissolve in ethanol, a mixture of water and ethanol was used as the solvent, thus successfully giving the expected single-crystals. All crystallizations of *p*-HOBA and different organic bases were carried out in a 1:1 ratio, considering the acid–base reaction stoichiometric ratio. For preparation of **1**, **2** and **3**, since selected bases of diethylamine, *tert*-butylamine and cyclohexylamine are all liquids with densities smaller than those of the mixed  $\text{H}_2\text{O}$ – $\text{C}_2\text{H}_5\text{OH}$  solution, they were carefully layered onto the mixed solvents. Three test tubes were used to facilitate the slow diffusion and desired single-crystals in all cases were obtained. For the preparation of **4** and **5**, *p*-HOBA was mixed directly with equivalent bases of imidazole or piperazine in  $\text{H}_2\text{O}$ – $\text{C}_2\text{H}_5\text{OH}$  solutions, which were allowed to evaporate at ambient condition to give the final crystalline products.

*Analytical and spectral data for the synthesized compounds*

[*p*-HOBAA<sup>-</sup>]·[protonated diethylamine] (**1**). M.p. 215 °C; Anal. Calcd. for  $\text{C}_{11}\text{H}_{17}\text{NO}_3$  ( $M_r = 211.26$ ): C, 62.5; H, 8.1; N, 6.6 %. Found: C, 62.4; H, 8.0; N, 6.5 %. IR (KBr,  $\text{cm}^{-1}$ ): 3421 *m*, 2993 *vs*, 2770 *vs*, 2658 *vs*, 2484 *vs*, 1626 *vs*, 1501 *vs*, 1377 *vs*, 1279 *vs*, 1160 *s*, 1091 *m*, 857 *s*, 784 *vs*, 701 *m*, 617 *s*.



[p-HOBAA<sup>-</sup>]·[protonated tert-butylamine] (**2**). M.p 260 °C; Anal. Calcd. for C<sub>11</sub>H<sub>17</sub>NO<sub>3</sub> ( $M_r = 211.26$ ): C, 62.5; H, 8.1; N, 6.6 %. Found: C, 62.3; H, 8.0; N, 6.45 %. IR (KBr, cm<sup>-1</sup>): 3418 *m*, 3103 *vs*, 3017 *vs*, 2829 *vs*, 2735 *s*, 2626 *s*, 2535 *m*, 1605 *vs*, 1502 *vs*, 1394 *vs*, 1287 *vs*, 1164 *s*, 1099 *m*, 856 *m*, 792 *m*, 703 *w*, 619 *m*.

[p-HOBAA<sup>-</sup>]·[protonated cyclohexylamine] (**3**). M.p. 220 °C; Anal. Calcd. for C<sub>13</sub>H<sub>19</sub>NO<sub>3</sub> ( $M_r = 237.29$ ): C, 65.8; H, 8.1; N, 5.9 %. Found: C, 65.7; H, 7.9; N, 5.7 %. IR (KBr, cm<sup>-1</sup>): 3420 *m*, 2938 *vs*, 2858 *s*, 2654 *vs*, 2572 *m*, 2141 *m*, 1597 *vs*, 1501 *vs*, 1439 *vs*, 1376 *vs*, 1276 *vs*, 1233 *vs*, 1156 *s*, 1091 *s*, 1030 *s*, 922 *w*, 892 *m*, 842 *s*, 788 *s*, 701 *w*, 644 *w*, 616 *m*.

[p-HOBAA<sup>-</sup>]·[protonated imidazole] (**4**). M.p. 224 °C; Anal. Calcd. for C<sub>10</sub>H<sub>10</sub>N<sub>2</sub>O<sub>3</sub> ( $M_r = 206.20$ ): C, 58.2; H, 4.9; N, 13.6 %. Found: C, 58.0; H, 4.6; N, 13.35 %. IR (KBr, cm<sup>-1</sup>): 3427 *s*, 3161 *vs*, 2922 *s*, 2803 *s*, 2689 *s*, 2026 *w*, 1598 *vs*, 1607 *vs*, 1542 *s*, 1390 *vs*, 1245 *vs*, 1160 *m*, 1128 *m*, 1049 *m*, 844 *s*, 780 *s*, 753 *m*, 697 *w*, 624 *m*.

[p-HOBA]<sup>-</sup>·[piperazine]<sup>-</sup>·H<sub>2</sub>O (**5**). M.p. 235 °C; Anal. Calcd. for C<sub>9</sub>H<sub>13</sub>NO<sub>4</sub> ( $M_r = 199.20$ ): C, 54.3; H, 6.6; N, 7.0 %. Found: C, 54.1; H, 6.4; N, 6.9%. IR (cm<sup>-1</sup>): 3132 *vs*, 3016 *vs*, 2773 *m*, 2497 *m*, 1611 *vs*, 1545 *s*, 1398 *vs*, 1271 *m*, 1228 *m*, 1165 *m*, 1095 *s*, 980 *m*, 856 *m*, 783 *m*, 697 *w*, 625 *m*.

#### *Molecular and supramolecular structure of **1***

The hydrogen bonds for **1** are listed in Table II, together with the hydrogen-bond information for **2–5**. Some C–H···π and π···π interactions for **1–5** are listed in Table III.

TABLE II. Hydrogen bond lengths (Å) and angles (°) for compounds **1–5**

Compound	D–H···A	Symmetry code	D···A	∠D–H···A
<b>1</b>	O(1)–H(2)···O(3)	−1/2+x, y, 1/2−z	2.6404	169.25
	N(1)–H(4)···O(2)	−1/2+x, 1/2−y, −z	2.8764	140.49
	N(1)–H(4)···O(3)	−1/2+x, 1/2−y, −z	3.0353	154.77
	N(1)–H(10)···O(2)	1/2−x, −1/2+y, z	2.7307	171.82
<b>2</b>	N(1)–H(1)···O(2)	—	2.8351	168.63
	N(1)–H(2)···O(2)	1−x, 1−y, −z	2.8422	161.42
	N(1)–H(3)···O(1)	2−x, 1−y, −z	2.7945	174.50
	O(3)–H(3B)···O(1)	2−x, −1/2+y, 1/2−z	2.6209	163.31
	C(3)–H(3A)···O(3)	1−x, 1/2+y, 1/2−z	3.2161	130.00
<b>3</b>	N(1)–H(1)···O(1)	1−x, −y, 1−z	2.8436	169.53
	N(1)–H(2)···O(2)	−x, −y, 1−z	2.8297	178.11
	N(1)–H(3)···O(2)	1+x, y, z	2.8752	155.38
	O(3)–H(3A)···O(1)	−x, 1/2+y, 1/2−z	2.6227	171.57
	C(9)–H(9A)···O(3)	x, ½−y, 1/2+z	3.2757	144.49
<b>4</b>	N(1)–H(1B)···O(1)	—	3.0681	120.62
	N(1)–H(1B)···O(2)	—	2.6888	177.11
	N(2)–H(2B)···O(1)	1−x, −1/2+y, 1/2−z	2.7580	154.02
	O(3)–H(3A)···O(1)	−x, 1/2+y, 1/2−z	2.6394	169.18



TABLE II. Continued

Compound	D-H···A	Symmetry code	D···A	$\angle$ D-H···A
<b>4</b>	C(9)–H(9A)···O(3)	$1+x, -1+y, z$	3.2810	138.77
	C(10)–H(10A)···O(2)	$x, 1/2-y, -1/2+z$	3.0467	119.88
<b>5</b>	O(2)–H(1)···N(1)	$x, 1/2-y, 1/2+z$	2.7446	154.23
	N(1)–H(1B)···O(3)	—	2.6270	88.21
	O(1)–H(2)···O(1W)	$-1+x, 1/2-y, -1/2+z$	2.7190	169.69
	O(1W)–H(3)···O(2)	$1-x, 1/2+y, 1/2-z$	2.8184	158.14
	O(1W)–H(4)···O(3)	—	2.8126	168.19

TABLE III. Data about C–H··· $\pi$  and  $\pi$ ··· $\pi$  interactions for compounds **1–5**

Cpd.	C–H··· $\pi$ or $\pi$ ··· $\pi$	Symmetry code	C···Cg <sup>a</sup> or Cg···Cg distance, Å	Perpendicular distance between planes of the rings, Å	$\angle$ C–H···Cg, °
<b>1</b>	C(8)–H(1)···Cg(1)	$-1/2+x, y, 1/2-z$	3.600	—	122.20
	C(9)–H(6)···Cg(1) <sup>b</sup>	—	3.522	—	97.91
	C(9)–H(7)···Cg(1)	—	3.522	—	117.07
	C(8)–H(17)···Cg(1)	$-1/2+x, y, 1/2-z$	3.600	—	97.07
<b>2</b>	C(9)–H(9B)···Cg(1)	$x, 1+y, z$	4.095	—	165.60
<b>3</b>	C(14)–H(14B)···Cg(1)	—	3.624	—	128.72
<b>4</b>	Cg(1)···Cg(1)	$1-x, -y, 1-z$	3.808	3.525	—
	Cg(1)···Cg(2) <sup>c</sup>	$1-x, 1-y, 1-z$	3.762	3.576	—
	Cg(2)···Cg(1)	$1-x, 1-y, 1-z$	3.762	3.451	—
<b>5</b>	C(8)–H(8B)···Cg(2)	—	3.788	—	147.40

<sup>a</sup>Cg denotes a center of an aromatic ring; in **1**, **2** and **3**; <sup>b</sup>Cg(1) denotes the phenyl ring; in **4**, imidazole ring;  
<sup>c</sup>Cg(2) denotes the phenyl ring

As depicted in Fig. 1a, the *p*-HOBA molecule has donated its carboxyl proton to the amino-nitrogen atom of diethylamine, resulting in molecule **1** consisting of a *p*-HOBAA<sup>−</sup> and a protonated diethylamine cation. The unit cell of **1** contains eight *p*-HOBAA<sup>−</sup>s and eight protonated diethylamine cations, which are connected together through hydrogen bonds and the electrostatic effect. After deprotonation, the two carboxyl C–O bond lengths in *p*-HOBAA<sup>−</sup> become similar (C(7)–O(2) 1.253(3) and C(7)–O(3) 1.264(3) Å) as opposed to the C–O bond lengths (1.322(2) and 1.228(2) Å) in an independent *p*-HOBA molecule,<sup>23</sup> indicating that the conjugative effect becomes stronger among the O(2), C(7) and O(3) atoms. This situation can also be found in **2–4**. In *p*-HOBAA<sup>−</sup>, the atoms O(1) and C(7) together with the phenyl ring define a plane *P*1. In the diethylamine cation, the atoms N(1), C(8), C(9) and C(10) define another plane *P*2. The dihedral angle between *P*1 and *P*2 is 78.01°. Through strong O(1)–H(2)···O(3) hydrogen bonds (see Table II for details), the *p*-HOBAA<sup>−</sup> molecules are connected to each other with a head-to-tail motif and thus, a zigzag 1D chain is formed, run-



ning along the *a*-axis direction (Figs. 1b and 1c). Between two adjacent 1D chains, a repeating unit exists which is composed of two pairs of *p*-HOBAA<sup>-</sup> molecules, which arrange in a parallel and antiparallel orientation, with the center-to-center distances between two parallel phenyl rings being 11.843 and 13.947 Å, respectively. The two non-parallel phenyl rings are almost perpendicular, with the dihedral angle being 89.23°. At each pair of inflexion points between two adjacent 1D chains, two *p*-HOBAA<sup>-</sup> molecules are held together by two diethylamine cations *via* N(1)–H(4)…O(2), N(1)–H(4)…O(3) and N(1)–H(10)…O(2) bonds (see Table II for details). As a result, a 2D network is formed, as depicted in Fig. 1b. These 2D undulated arrays (Fig. 1c) are further stabilized by four types of interlayer C–H…π interactions (see Table III for details).

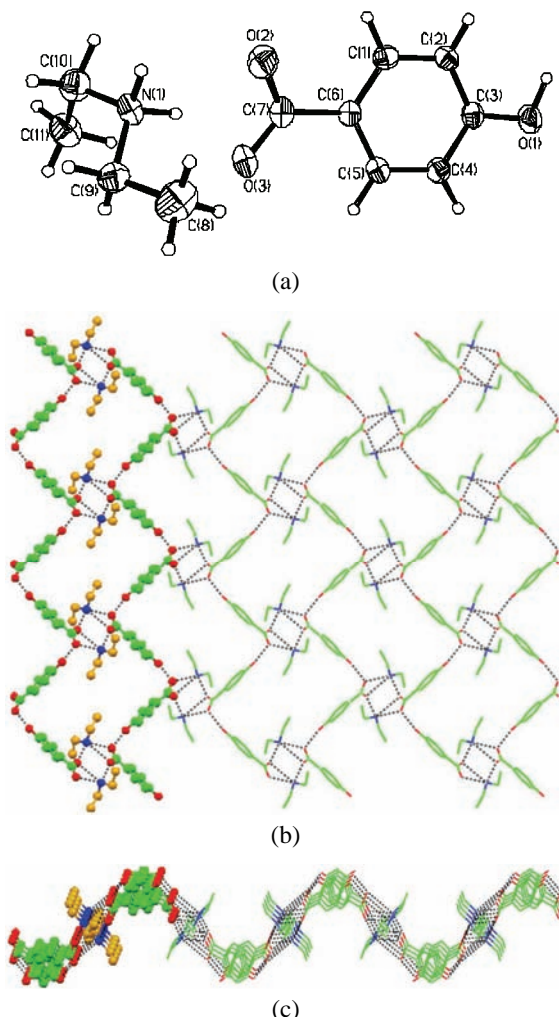


Fig. 1. a) Molecular structure of **1** with atomic numbering; 1D chain along the *a*-axis direction and perspective view in the *ac* plane (b) and in the *bc* plane (c).

### Molecular and supramolecular structure of **2**

Just as in compound **1**, *p*-HOBA molecule in **2** also transfers its carboxyl proton to the amino-nitrogen atom of *tert*-butylamine, resulting in molecule **2** consisting of a *p*-HOBAA<sup>-</sup> and a protonated *tert*-butylamine cation (Fig. 2a). A unit cell of **2** contains four pairs of *p*-HOBAA<sup>-</sup> and protonated *tert*-butylamine cation which connected together through hydrogen bonds and electrostatic effect. Similar to **1**, compound **2** also possesses abounding strong N–H···O and O–H···O hydrogen bonds. Primarily, the molecular assembly among *p*-HOBAA<sup>-</sup> occurs through O(3)–H(3B)···O(1) interactions, resulting in a zigzag 1D chain structure. Such a 1D chain runs along the *b*-axis with the *p*-HOBAA<sup>-</sup> moieties arranging in a head-to-tail motif (Fig. 2b). Between two contiguous 1D arrays, being similar to that in **1**, a repeating unit is found containing two pairs of *p*-HOBAA<sup>-</sup>, which

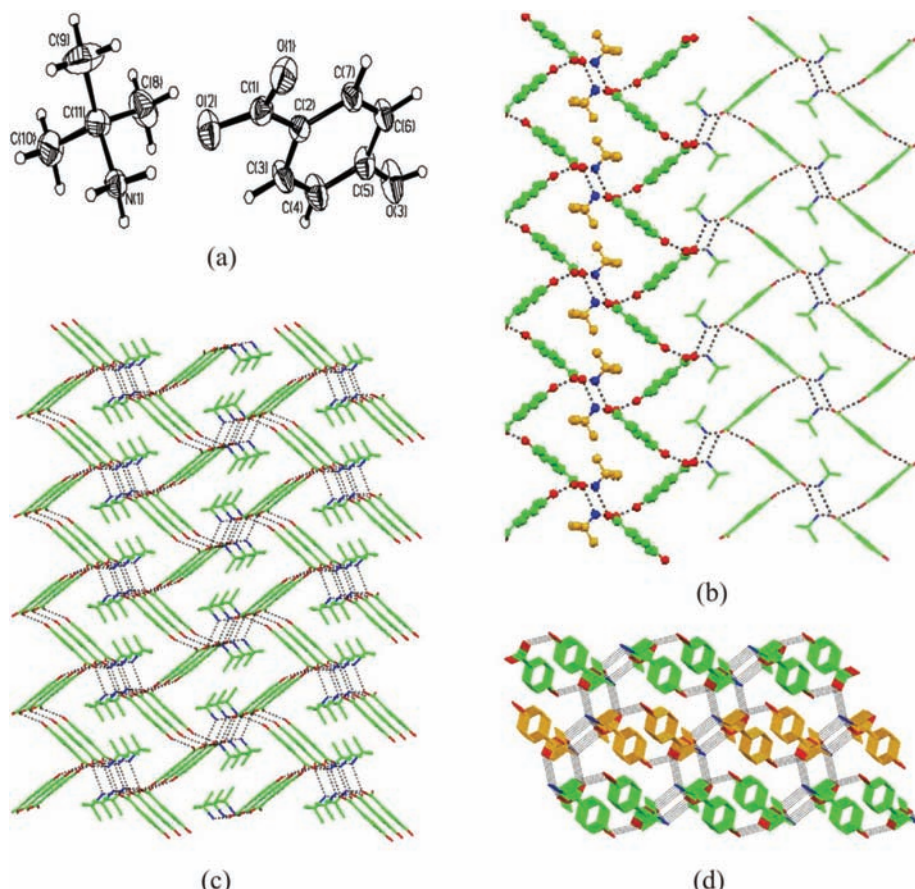


Fig. 2. a) Molecular structure of **2** with atomic numbering; b) 1D chain along the *b*-axis direction and perspective view in the *bc* plane ; 3D architecture in the *bc* plane (c) and in the *ac* plane (d).

arrange in a parallel and antiparallel orientation (Fig. 2b), with the center-to-center distances between two parallel phenyl rings being 8.666 and 15.746 Å, respectively. The dihedral angle between two non-parallel phenyl rings is 81.64°. Then, these 1D chains are linked together by protonated *tert*-butylamine cations *via* N(1)–H(1)…O(2) and N(1)–H(2)…O(2) interactions (Table II). As depicted in Fig. 2b, two protonated *tert*-butylamine cations combine two *p*-HOBA<sup>−</sup> molecules together at each pair of inflection points between two adjacent 1D chains and thus, a 2D hydrogen-bonded net is given in the *bc* plane. Further analysis shows that these 2D layers adopt a parallel stack along the *a*-axis *via* N(1)–H(3)…O(1) and finally create a 3D supramolecular architecture (Figs. 2c and 2d), which is distinct from that of **1**. In addition, interlayer C(3)–H(3A)…O(3) and intra-layer C(9)–H(9B)…Cg(1) (Cg(1) denotes phenyl ring) (see Table II and Table III for details) forces also help to stabilize the whole supramolecular system.

#### *Molecular and supramolecular structure of **3***

Compound **3** comprises a *p*-HOBA<sup>−</sup> and a protonated cyclohexylamine cation (Fig. 3a). The unit cell of **3** contains four pairs of *p*-HOBA<sup>−</sup> and a protonated cyclohexylamine cation. The supramolecular constructions in **3** are very similar to those in **2**. Firstly, through O(3)–H(3A)…O(1) interactions, a zigzag 1D chain along the *b*-axis direction is formed of *p*-HOBA<sup>−</sup> molecules in a head-to-tail fashion (Fig. 3b), and in the two neighboring 1D chains, two pairs of *p*-HOBA<sup>−</sup> molecules array mutually parallel but reversed (Fig. 3b). Then, *via* N(1)–H(2)…O(2) and N(1)–H(3)…O(2) interactions, protonated cyclohexylamine cations join these 1D chains together at each pair of inflection points to make a 2D layer network in the *bc* plane (Fig. 3b), with two protonated cyclohexylamine cations connecting two *p*-HOBA<sup>−</sup> anions. Ultimately, the 2D layers stack along the *a*-axis *via* N(1)–H(1)…O(1) interactions to generate a 3D supramolecular architecture (Fig. 3c). However, opposed to **2**, in **3**, C(9)–H(9A)…O(3) forces exist in the same 2D layer, while C(14)–H(14B)…Cg(1) (see Table III) interactions are observed between neighboring 2D layers, both of which stabilize the supramolecular structure of **3**. In addition, in the contiguous 1D chains of **3**, the center-to-center distances between two pairs of parallel phenyl rings are 10.537 and 15.833 Å, respectively, both of which are larger than the corresponding values in **2**. The dihedral angle between two non-parallel phenyl rings is 46.23°, which is also different from that in **2**. These distinctions may be ascribed to the volume of the protonated cyclohexylamine cation being larger than that of the protonated *tert*-butylamine cation.

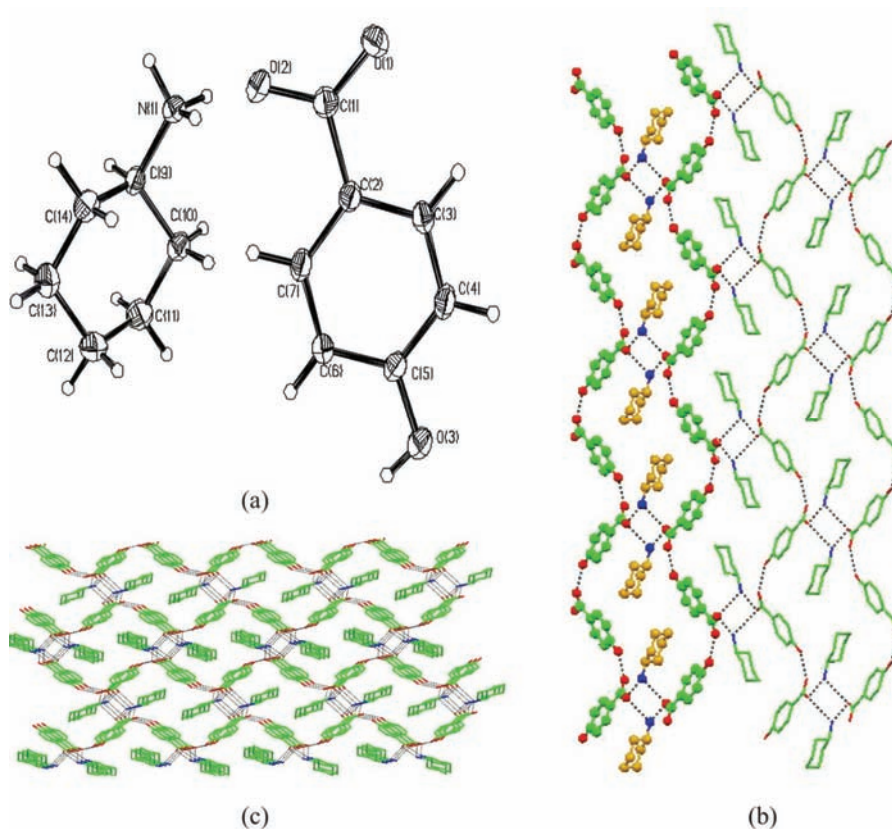


Fig. 3. a) Molecular structure of **3** with atomic numbering; b) 1D chain along the *b*-axis direction and perspective view in the *bc* plane; c) 3D structure viewed along the *a*-axis.

#### *Molecular and supramolecular structure of **4***

Compound **4** (Fig. 4a) is made up of a *p*-HOBA<sup>−</sup> and protonated imidazole cation. A unit cell contains four *p*-HOBA<sup>−</sup>s and four protonated imidazole cations. With respect to the supramolecule building of **4**, similar to **1**, **2** and **3**, 1D zig-zag chains are primarily formed *via* O(3)–H(3A)…O(1) interactions between *p*-HOBA<sup>−</sup> molecules with a head-to-tail motif (Fig. 4b). However, between the two neighboring 1D chains, as the repeat unit, two pairs of parallel *p*-HOBA<sup>−</sup>s array in the same direction (Fig. 4b), respectively, which is a significant difference from those in **1**, **2** and **3**. In addition, for the repeat unit, both center-to-center distances between two pairs of parallel phenyl rings are the same and equal to 9.616 Å, and the dihedral angle between two non-parallel phenyl rings is 46.23°, which are also distinct to those in **1**, **2**, and **3**. As a consequence, when the 1D chains are held together by protonated imidazole cations through N(1)–H(1B)…O(1) and N(1)–H(1B)…O(2), as well as N(2)–H(2B)…O(1) interactions

(see Table II), a diverse 2D network is produced. In the 2D net, each inflection point of each 1D chain connects with a pair of protonated imidazole cations and this pair of protonated imidazole cations couple with two inflection points of another adjacent 1D chain synchronously. Further inspection of the lattice arrangement reveals that both C-H···O and face-to-face interactions stabilize the supramolecular architecture. Among them, C(9)-H(9A)···O(3) is intralayered, while C(10)-H(10A)···O(2) joins the interlayer acid and base components. Two types of  $\pi$ ··· $\pi$  stackings between phenyl ring-to-phenyl ring and phenyl ring-to-imidazole ring (see Table III for details) are also interlayer interactions.

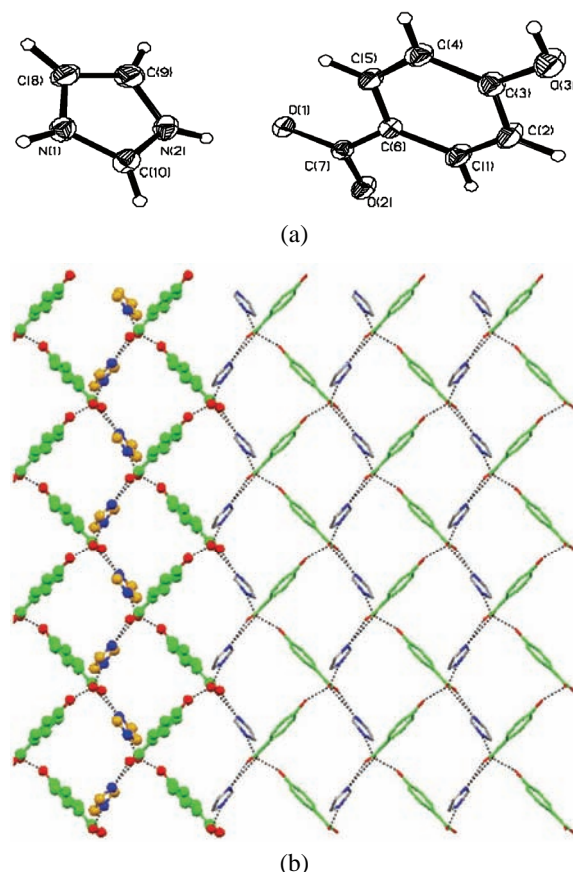


Fig. 4. a) Molecular structure of **4** with atomic numbering; b) 1D chain along the *b*-axis direction and 2D network viewed along the *c*-axis.

In view of the 2D structure of **4** being different from those of **1–3**, one can find that the organic base of imidazole in **4** has two important structural characteristics distinct from those of the organic bases used in **1–3**. One is that it is a rigid aromatic base and the other that it has two nitrogen atoms, which means that each protonated imidazole cation can form hydrogen bonds from two dif-

ferent directions of the molecule. On the contrary, in **1–3**, the organic bases are not rigid aromatic bases and they have only one nitrogen atom. It is possible that these two significant features of imidazole finally produce the unique 2D supramolecular building of **4**.

#### *Molecular and supramolecular structure of **5***

Opposed to **1–4**, co-crystallization of piperazine with *p*-HOBA yields the neutral molecular co-crystal **5**, in which *p*-HOBA does not transfer its carboxyl hydrogen atom to the piperazine molecule (Fig. 5a). Additionally, a lattice water solvent molecule is observed in **5**; hence compound **5** is built up of a *p*-HOBA, a piperazine and a water molecule. The unit cell contains four *p*-HOBA, two piperazine and four water molecules. In each *p*-HOBA, the bond distances of C–O are 1.259(3) and 1.273(2) Å, respectively, which are also different from those in an independent *p*-HOBA molecule.<sup>23</sup> As for the supramolecular building of **5**, first, each piperazine acts as a hydrogen-bonding connector, joining four *p*-HOBA subunits *via* strong pair-wise O(2)–H(1)…N(1) and N(1)–H(1B)…O(3) bonds (see Table II for details) and two *p*-HOBA molecules are linked to two piperazine molecules. Thus, a tape-like 1D supramolecular motif is formed, running along the *a*-axis direction, as shown in Fig. 5b. Then, each water molecule acts as a 3-connector to link with three *p*-HOBA molecules through O(1)–H(2)…O(1W), O(1W)–H(3)…O(2) and O(1W)–H(4)…O(3), which results in the 1D tapes being combined and a 3D hydrogen-bonding network being finally formed (Fig. 5c). Within the 3D network, an intermolecular C(8)–H(8B)…Cg(2) force is observed, which aids in the stabilization of the whole crystal structure.

#### *Melting point of compounds **1–5***

The melting point of *p*-HOBA is 213 °C. Of the five bases studied here, diethylamine, *tert*-butylamine and cyclohexylamine are all liquids and the melting points of imidazole and piperazine are 90 and 106 °C, respectively. The experimentally determined melting points for **1–5** are 215, 260, 220, 224 and 235 °C, respectively. It is evident that all the compounds **1–5** have higher melting points than their corresponding reactants, which may be because the hydrogen-bond types and numbers in **1–5** are greater than those in the corresponding reactants. For instance, the N–H…O hydrogen bond exists universally in **1–5**, while it cannot be found in any of the reactants used in this study. On the other hand, comparisons of the strength of the hydrogen bonds and the C–H…O, C–H…π and π…π interactions (given in Tables II and III) and the melting points suggest that the melting points of the complexes are influenced not only by hydrogen bonds and other interactions. For instance, for **2**, **3** and **5**, although they all have four hydrogen bonds and one C–H…π interaction, and the distance C…Cg in **2** of 4.095 Å is the longest, the three of them have different melting points and the melting point of **2** is the highest. The maximum supramolecular number of interactions, including

six hydrogen bonds and three other interactions, exist in **4**, but the melting point of **4** is not the highest of the five complexes. Compound **1** contains four hydrogen bonds and four other interactions, which is more than in compounds **2**, **3** and **5**, however, its melting point is the lowest. Most important, the higher melting points suggest that compounds **1–5** are not the ordinary superposition of the reactants and that they became new materials different from the original reactants, and that they are more stable than the reactants, which might be useful information for further investigations on the synthesis of new pattern functional materials.

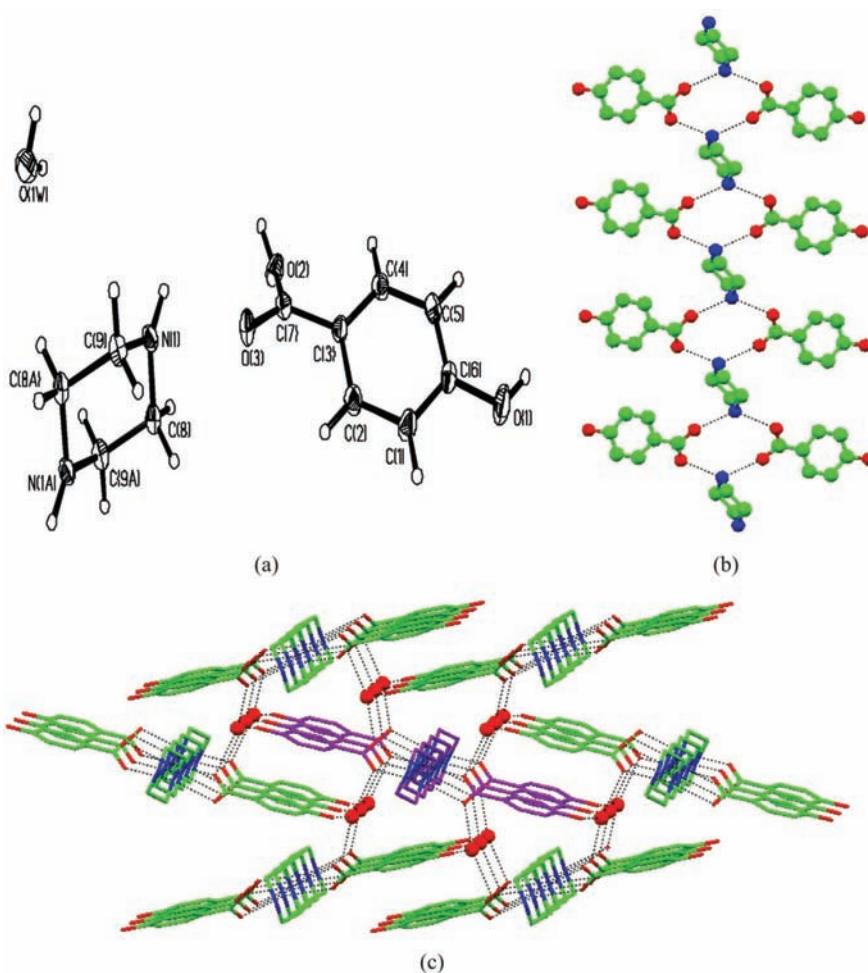


Fig. 5. a) Molecular structure of **5** with atomic numbering; b) 1D tape along the *a*-axis; c) 3D structure viewed along the *a*-axis.

## CONCLUSIONS

Five acid–base complexes were synthesized using *p*-hydroxybenzoic acid (*p*-HOBA) as the building block, which form 2D and 3D net works through hydrogen bonds and C–H···O, C–H··· $\pi$  and  $\pi$ ··· $\pi$  interactions. Determination of their melting points showed that the five compounds are more stable than their respective reactants, that they are not the ordinary superposition of the reactants and that they became new materials different from the original reactants.

*Supplementary material.* CCDC-652250 for **1**, 651984 for **2**, 651983 for **3**, 691985 for **4** and 651986 for **5** contain the supplementary crystallographic data for this paper. These data can be obtained free of charge at [www.ccdc.cam.ac.uk/conts/retrieving.html](http://www.ccdc.cam.ac.uk/conts/retrieving.html) (or from the Cambridge Crystallographic Data Centre (CCDC), 12 Union Road, Cambridge CB2 1EZ, UK; fax: +44(0)1222-336033; email: deposit@ccdc.cam.ac.uk).

*Acknowledgements.* This work was supported by the Natural Science Foundation of the Shandong Province (No. Z2007B01 and Y2007B14) and by the Doctoral Fund of Qingdao, University of Science and Technology.

### ИЗВОД

ПРОЈЕКТОВАЊЕ КРИСТАЛА КИСЕЛИНСКО–БАЗНИХ КОМПЛЕКСА СА 2D И 3D  
ВОДОНИЧНО ВЕЗАНИМ СИСТЕМИМА КОРИШЋЕЊЕМ *p*-ХИДРОКСИБЕНЗОЕВЕ  
КИСЕЛИНЕ КАО ГРАДИВНОГ БЛОКА

PU SU ZHAO, XIAN WANG, FANG FANG JIAN, JUN LI ZHANG и HAI LIAN XIAO

*New Materials and Function Coordination Chemistry Laboratory, Qingdao University of Science and Technology, Qingdao Shandong 266042, P. R. China*

*p*-Хидроксibenзоева киселина (*p*-НОВА) је изабрана као елемент за самоизградњу са пет база: диетиламином, *tert*-бутиламином, циклохексиламином, имидазолом и пиперазином градећи одговарајуће киселинско–базне комплексе **1–5**. Кристално-структурне анализе указују да се протон-трансфер са карбоксиленог водоника на азотов атом базе може уочити код **1–4**, а само у **5** молекул из растварача воде коегзистира са *p*-НОВА и пиперазином. Водоничним везама О–Н···О, присутним у **1–4**, депротоновани *p*-хидроксibenзоатни анјони *p*-НОВАА<sup>–</sup> се једноставно повезују мотивом глава–реп градећи једнодимензионалне (1D) низове додатно проширене на разне дводимензионалне (2D) (за **1** и **4**) и тродимензионалне (3D) (за **2** и **3**) мреже путем N–H···O интеракција. Док су у **5** неутрална киселина и база повезане паровима О–Н···N и N–H···O веза градећи 1D траку, комбинацијом 1D трака са молекулима воде креира се 3D мрежа. Неке C–H···O, C–H··· $\pi$  и  $\pi$ ··· $\pi$  интеракције изван и унутар слојева помажу стабилизовању супрамолекуларних творевина. Тачке топљења указују да **5** киселинско–базних комплекса нису обична суперпозиција реактаната и да су стабилнији од оригиналних реактаната.

(Примљено 16. априла, ревидирано 21. септембра 2009)

### REFERENCES

1. X. L. Zhang, X. M. Chen, *Cryst. Growth Des.* **5** (2005) 617
2. D. Y. Kong, J. L. McBee, A. Clearfield, *Cryst. Growth Des.* **5** (2005) 643
3. M. Du, Z. H. Zhang, X. J. Zhao, *Cryst. Growth Des.* **5** (2005) 1199

4. Z. J. Li, Y. Abramov, J. Bordner, J. Leonard, A. Medek, A. V. Trask, *J. Am. Chem. Soc.* **128** (2006) 8199
5. S. Wishkerman, J. Bernstein, M. B. Hickey, *Cryst. Growth Des.* **9** (2009) 3204
6. P. Gilli, L. Pretto, V. Bertolasi, G. Gilli, *Acc. Chem. Res.* **42** (2009) 33
7. L. S. Reddy, S. K. Chandran, S. George, N. J. Babu, A. Nangia, *Cryst. Growth Des.* **7** (2007) 2675
8. A. Nangia, *Cryst. Growth Des.* **8** (2008) 1079
9. M. Khan, V. Enkelmann, G. Brunklaus, *Cryst. Growth Des.* **9** (2009) 2354
10. A. M. Beatty, *Coord. Chem. Rev.* **246** (2003) 131
11. B. R. Bhogala, P. Vishweshwar, A. Nangia, *Cryst. Growth Des.* **2** (2002) 325
12. B. R. Bhogala, A. Nangia, *Cryst. Growth Des.* **3** (2003) 547
13. M. Eddaaoudi, D. B. Moler, H. Li, B. Chen, T. M. Reineke, M. O'Keeffe, O. M. Yaghi, *Acc. Chem. Res.* **34** (2001) 319
14. P. J. Hagrman, D. Hagraman, J. Zubieta, *Angew. Chem., Int. Ed.* **38** (1999) 2638 and references therein
15. M. Du, Z. H. Zhang, X. G. Wang, H. F. Wu, Q. Wang, *Cryst. Growth Des.* **6** (2006) 1867
16. F. F. Jian, P. S. Zhao, Q. X. Wang, *Chin. J. Struct. Chem.* **24** (2005) 184
17. L. H. Wei, *Acta Crystallogr. E* **62** (2006) o4506
18. Y. Moritani, N. Sasahara, S. Kashino, M. Haisa, *Acta Crystallogr. C* **43** (1987) 154
19. H. Parshad, K. Frydenvang, T. Liljefors, H. O. Sorensen, C. Larsen, *Int. J. Pharm.* **269** (2004) 157
20. C. B. Aakeroy, G. S. Bahra, P. B. Hitchcock, Y. Patell, K. R. Seddon, *Chem. Commun.* (1993) 152
21. G. M. Sheldrick, *SHELXTL, v5 Reference Manual*, Siemens Analytical X-Ray Systems, Madison, WI, 1997
22. A. J. Wilson, *International Table for X-Ray Crystallography*, Vol. C, Kluwer Academic, Dordrecht, 1992, Tables 6.1.1.4 (pp. 500–502) and 4.2.6.8 (pp. 219–222)
23. M. Colapietro, A. Domenicano, C. Marciante, *Acta Crystallogr. B* **35** (1979) 2177.